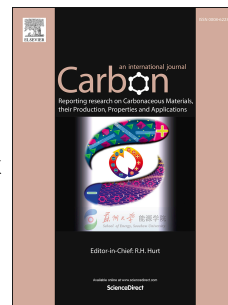


Journal Pre-proof

Low Energy Consumption Flow Capacitive Deionization with a Combination of Redox Couples and Carbon Slurry

Qiang Wei, Yudi Hu, Jian Wang, Qiang Ru, Xianhua Hou, Lingzhi Zhao, Denis.Y.W. Yu, Kwan San Hui, Dongliang Yan, Kwun Nam Hui, Fuming Chen



PII: S0008-6223(20)30704-1

DOI: <https://doi.org/10.1016/j.carbon.2020.07.044>

Reference: CARBON 15514

To appear in: *Carbon*

Received Date: 3 June 2020

Revised Date: 21 July 2020

Accepted Date: 24 July 2020

Please cite this article as: Q. Wei, Y. Hu, J. Wang, Q. Ru, X. Hou, L. Zhao, D.Y.W. Yu, K. San Hui, D. Yan, K.N. Hui, F. Chen, Low Energy Consumption Flow Capacitive Deionization with a Combination of Redox Couples and Carbon Slurry, *Carbon*, <https://doi.org/10.1016/j.carbon.2020.07.044>.

This is a PDF file of an article that has undergone enhancements after acceptance, such as the addition of a cover page and metadata, and formatting for readability, but it is not yet the definitive version of record. This version will undergo additional copyediting, typesetting and review before it is published in its final form, but we are providing this version to give early visibility of the article. Please note that, during the production process, errors may be discovered which could affect the content, and all legal disclaimers that apply to the journal pertain.

© 2020 Elsevier Ltd. All rights reserved.

Qiang Wei: Device design, Experiment methodology, Data analysis, Original draft reparation

Yudi Hu: Experiment methodology

Jian Wang: Device design

Qiang Ru: Discussion on the electrochemical experiments

Xianhou Hou: Primarily developed the present work, Investigation, Data analysis, Paper writing

Lingzhi Zhao: The electrochemical analysis, Paper writing

Denis Y. W. Yu: Reviewing and Editing

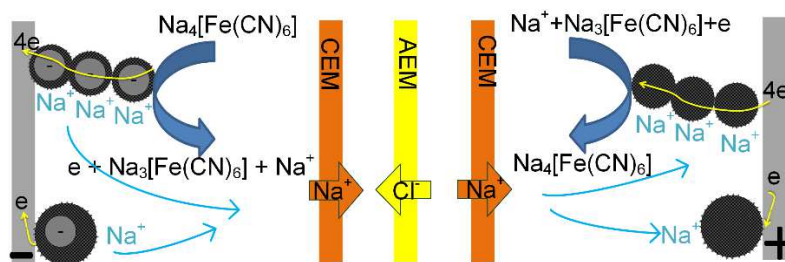
Kwan San Hui: Paper writing and Editing

Dongliang Yan: Discussion and analysis of the supplemented experiments

Kwun Nam Hui: Primarily developed the present work, Data analysis, Paper writing

Fuming Chen: conceptualized the work, Data analysis, wrote the paper, Supervision

By the introduction of redox couples to flow capacitive deionization, the continuous desalination process is achieved with a high salt removal rate and low energy consumption.



Journal Pre-proof

1 **Low Energy Consumption Flow Capacitive Deionization with a Combination of**
2 **Redox Couples and Carbon Slurry**

3 Qiang Wei¹, Yudi Hu¹, Jian Wang¹, Qiang Ru¹, Xianhua Hou^{1,2*}, Lingzhi Zhao^{1,2}, Denis Y.
4 W. Yu³, Kwan San Hui⁴, Dongliang Yan⁵, Kwun Nam Hui^{6*}, Fuming Chen^{1,2*}

5 ¹ *Guangdong Provincial Key Laboratory of Quantum Engineering and Quantum Materials,*
6 *Guangdong Engineering Technology Research Center of Efficient Green Energy and*
7 *Environment Protection Materials, School of Physics and Telecommunication Engineering,*
8 *South China Normal University, Guangzhou 510006* houxianhua@m.scnu.edu.cn,
9 fmchen@m.scnu.edu.cn

10 ² *SCNU Qingyuan Institute of Science and Technology Innovation Co., Ltd., Qingyuan*
11 *511517, China*

12 ³ *School of Energy and Environment, City University of Hong Kong, Tat Chee Avenue,*
13 *Kowloon, Hong Kong Special Administrative Region*

14 ⁴ *Engineering, Faculty of Science, University of East Anglia, Norwich, UK*

15 ⁵ *School of Material Science and Engineering, Guilin University of Electronic Technology,*
16 *Guilin, 541004, China*

17 ⁶ *Joint Key Laboratory of the Ministry of Education, Institute of Applied Physics and*
18 *Materials Engineering, University of Macau, Avenida da Universidade, Taipa, Macau, PR*
19 *China* bizhui@umac.mo

20
21 **Abstract:** Flow-electrode capacitive deionization (FCDI) is a new sustainable desalination
22 technology where continuous desalination can be achieved by the electro dialysis coupling
23 method. However, its development is hindered owing to high energy consumption and low
24 salt removal rate. Herein, by combining ferri-/ferrocyanide redox couple with flow activated
25 carbon (AC)/carbon black (CB) slurry, continuous desalination process is achieved with a
26 high salt removal rate of $1.31 \mu\text{g cm}^{-2} \text{ s}^{-1}$ and low energy consumption of $102.68 \text{ kJ mol}^{-1}$ at
27 the current density 2.38 mA cm^{-2} (50 mA current for a 21 cm^2 active area). The operating
28 voltage plateau can be reduced to 0.69 V when 10 wt% AC/CB (mass ratio of 9:1) is mixed

29 with 20 mM/20 mM ferri-/ferrocyanide as the flow electrodes, compared with more than 3 V
30 for only carbon flow or redox medium alone. The influences of carbon content and current
31 densities are further investigated to so that the performances can be controlled. This work
32 enables the development of energy-saving desalination systems by coupling FCDI with redox
33 desalination technique.

34 **Keywords:** Electrochemical desalination, Flow-electrode capacitive deionization, activated
35 carbon/carbon black, redox desalination

36 1. Introduction

37 With the increase in population, the scarcity of fresh water is becoming a serious problem[1].
38 Ocean is a huge water source and it is therefore imperative to obtain freshwater from the sea
39 by some effective desalination methods. Reverse osmosis and distillation are the matured
40 desalination technology. However, the desalination equipment system is very complicated and
41 expensive. Capacitive deionization (CDI) is a water flow desalination technology without the
42 high pressure applied[2-5]. Its advantages include high energy-efficiency, cost-effectiveness,
43 and eco-friendliness[6, 7]. When an electrical field is applied between the carbon electrodes,
44 the ions in the salt feed are adsorbed to purify the water. Traditional CDI utilizes static carbon
45 material as electrodes with only limited salt removal capacity of less than 20 mg g^{-1} , and
46 regeneration has to be carried out after salt absorption saturation [8, 9]. Therefore, flow-
47 electrode capacitive deionization (FCDI) has been introduced and rapidly developed recently
48 [8, 10-13]. Compared with the traditional CDI technology, the electro-active flow with
49 suspended carbon-based materials such as activated carbon, carbon nanotubes, or other
50 conductive agents in slurry form as flow electrodes enhances the electrochemical salt removal
51 capacity in FCDI [14-17]. Specifically, the suspended carbon black (CB) or activated carbon
52 (AC) slurry is allowed to flow in the two electrode streams, and the salt stream passed
53 through the middle compartment. This flow carbon electrode-based CDI exhibits an unlimited
54 salt removal capacity. Other host materials like the redox couples can be introduced into the
55 carbon flow electrode to enhance the charge transport as well as conductivity. Ma et. al.
56 demonstrated the mixture for organic-based redox couple into 1 wt% activated carbon
57 electrode in an aqueous medium which enhances the FCDI desalination performance [18].
58 The aqueous hydroquinone/benzoquinone was chosen as the redox species for desalination at
59 the constant voltage mode. However, hydroquinone or benzoquinone is dangerously toxic for
60 human. During the re-circulating redox reaction, their derivatives such as halobenzoquinones

61 may be generated in the stream chlorination. The initial salt feed with 2000 ppm was desalted
62 to 1000 ppm at the constant voltage of 1.2 V. The synergistic effect between the carbon and
63 redox couple played a key role to enhance the desalination performance further. The removal
64 rate and energy consumption are two key parameters in the FCDI. In order to achieve low
65 energy consumption and high removal rate, we propose to combine ferri-/ferrocyanide redox
66 couple with AC/CB slurry as FCDI electrodes. The redox couple can enhance the charge
67 transfer between the flowing electrodes and current collector. A low voltage plateau of 0.69 V
68 can be obtained in the combination of redox couples and slurry-type electrode which flow
69 through the positive and negative stream by re-circulation process. As a results, a salt removal
70 rate of $1.31 \mu\text{g cm}^{-2} \text{ s}^{-1}$ and energy consumption of $102.68 \text{ kJ mol}^{-1}$ can be obtained at the
71 current density 2.38 mA cm^{-2} (50 mA current and 21 cm^2 active area) with the mixture of 10
72 wt% AC/CB (mass ratio of 9:1) and 20 mM/20 mM ferri-/ferrocyanide as flow electrodes
73 during the continuous desalination process, where the plateau of the operating voltage can be
74 maintained at 0.69 V, compared with more than 3 V with only carbon flow or redox medium
75 alone. The enhanced performance of the FCDI is due to the synergetic effect of carbon flow
76 electrode and redox couple. We also found that the content of carbon electrodes greatly
77 affects the removal rate and energy consumption. This work highlights a route towards fast
78 desalination with the reduced energy consumption via the combination of redox couples and
79 carbon slurry, even under high current conditions.

80

81 **2. Experimental section:**

82 **2.1 Materials and cell design**

83 The activated carbon (specific surface area: $1301.3 \text{ m}^2 \text{ g}^{-1}$, particle size: $\sim 19 \mu\text{m}$) was ordered
84 from Yihuan Carbon Co., Ltd., Fuzhou, China, and carbon black (specific surface area: 190.2

85 $\text{m}^2 \text{g}^{-1}$, particle size: 12 μm) from Alfa Aesar. $\text{K}_3\text{Fe}(\text{CN})_6$ (99%) was purchased from Energy
86 Chemical, and $\text{K}_4\text{Fe}(\text{CN})_6$ ($\geq 99.5\%$) from Macklin. NaCl (99.5%) was brought from Aldrich.
87 The cell of redox flow FCDI was fabricated according to the following architecture as shown
88 in Figure 1a and Figure S1: graphite paper (JING LONG TE TAN, Beijing, 0.2 mm thickness)
89 as current collector | redox couples/carbon flow chamber || desalinated stream || brine stream ||
90 redox couples/carbon flow chamber | graphite paper as the current collector. The symbols of |
91 and || denote the compartment separation and membrane, respectively. The carbon flow
92 chambers were made of acrylic plates (130 mm \times 130 mm \times 2 mm) with a snake flow path (7
93 cm length, 2 mm width and 2 mm depth). Each carbon flow chamber has 15 flow paths. The
94 active area is 21 cm^2 in totally. Two pieces of cation exchange membrane (CEM, Tokuyama,
95 Japan) are placed between the salt stream and redox carbon flow chamber at both sides. One
96 piece of anion exchange membrane (AEM, Tokuyama, Japan) is located between brine and
97 desalination stream.

98 **2.2 Electrochemical measurement and desalination tests**

99 The electrochemical properties of redox couples was measured with a three-electrode cell by
100 cyclic voltammetry (CV) using an electrochemical workstation (CHI760E, CH Instruments,
101 Ins, USA) in 0.5 M NaCl electrolyte containing 20 mM/20 mM of $\text{K}_3\text{Fe}(\text{CN})_6$ and
102 $\text{K}_4\text{Fe}(\text{CN})_6$. The working electrode was a glassy carbon electrode with an exposed area with a
103 diameter of 3 mm, polished by the suspended Al_2O_3 in deionized water. Pt grid and standard
104 Ag/AgCl are used as the counter and reference electrode, respectively. The applied scan rate
105 was controlled at 5 $\text{mV}\cdot\text{s}^{-1}$ with the working window range from -0.1 to 0.5 V vs. Ag/AgCl .

106 The flow electrode material contains water with 10 wt % AC/CB (mass ratio of 9:1) carbon
107 slurry and 20 mM/20 mM of $\text{K}_3\text{Fe}(\text{CN})_6$ and $\text{K}_4\text{Fe}(\text{CN})_6$. 9000 ppm of NaCl was added to the
108 above solution to enhance the conductivity, and the total volume of solution is 160 ml. The

109 whole mixture is allowed to stir for two days prior to the experiment. The desalination and
 110 concentrate chambers (streams A and B) contain the same concentration of NaCl with 9000
 111 ppm in 80 mL initially. The desalination current was provided by the battery analyzer
 112 (Neware, Shenzhen, China) with a current of 10 mA, 30 mA, 50 mA, 70 mA or 90 mA at
 113 ambient temperature. The system was also tested with flow electrode with amount of different
 114 carbon slurry (i.e. 0, 1.11, 3.33, 5.56, 7.78 and 10 wt % AC/CB with mass ratio of 9:1). All
 115 the water flow was pumped at the rate of 8.1 ml min⁻¹. Before desalination, the solutions were
 116 kept under the flow condition for two hours without any applied current. The variation of salt
 117 concentrations in streams A and B were recorded by conductivity meters (EPU357, EDAQ,
 118 Australia).

119 2.3 Calculation Procedures

120 **The salt removal rate** (ASRR, $\mu\text{g cm}^{-2} \text{s}^{-1}$), which describes the desalination rate, can be
 121 calculated by the equation 1 [19, 20].

$$122 \quad \text{ASRR} = \frac{\left(\frac{\Delta c}{\Delta t} \times V\right)}{A_{\text{cell}}} \quad (1)$$

123 Where $\Delta c/\Delta t$ is the salt concentration change per second ($\Delta\text{ppm s}^{-1}$), V is the volume of the
 124 salt stream (80 mL) and A_{cell} is the cross-sectional area of the cell (21 cm^2) in this device.

125 **Charge efficiency** (Λ , %) is defined as the percentage ratio of salt removed to the applied
 126 electrons, which can be determined by the following formula:

$$127 \quad \Lambda = \frac{\text{ASRR} \times F}{60 \times 10^3 \times i \times M} \quad (2)$$

128 Where i is the current density (in mA cm^{-2}) and M is the molar mass of NaCl (58.44 g mol^{-1}).
 129 F is Faraday constant.

130 **Energy consumption** (E_c , kJ mole⁻¹) can be calculated as follows:

$$131 \quad \bar{E} = \frac{3.6\Delta E}{\left[(c_0 - c_f) \times \frac{V}{10^6 \times M} \right]} \quad (3)$$

132 Where ΔE is the total energy consumption (Wh) during charging, c_0 and c_f are the initial and
133 final NaCl concentrations in ppm, respectively.

134

135 **3. Results and discussion**

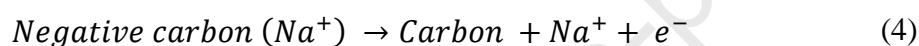
136 **3.1 The combination desalination mechanism of redox couples and carbon slurry**

137 The schematic representation of the FCDI device is shown in Figure 1a. All the compartments
138 are made of acrylic plates. The two end plates with 8 mm thickness are fastened with screws
139 to compactly support the device to avoid the leakage. The thicknesses of the other flow
140 compartments are 2 mm. The flow slurry electrodes are re-circulated using peristaltic pumps.
141 The flow electrode and the salt feed are recirculated independently. A proposed combination
142 mechanism is schematically demonstrated in Figure 1b-d for flow electrode with carbon only,
143 redox couples only and their synergetic combination.

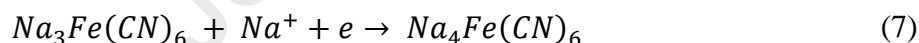
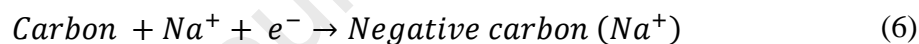
144 Figure 1b shows the desalination mechanism with carbon absorption. In the anode carbon
145 stream, the negative charged carbon releases an electron to the current collector and a sodium
146 ion to the neighbor salt stream through CEM, in which the sodium ion are obtained from the
147 cathode stream. This process is exactly the same as in the conventional FCDI or CDI. For the
148 case with only redox couple material in the flow electrode, as displayed in Figure 1c, the
149 desalination mechanism is based on the coupling electrolysis owing to the redox reaction of
150 redox couples. On the surface of the anode current collector, the oxidation reaction of
151 ferrocyanide occurs with the release of an electron to the outer circuit while the sodium ion is

152 transported to the neighbor salt stream through the CEM. At the cathode stream, ferricyanide
 153 is reduced to ferrocyanide with the acceptance of an electron from the outer circuit and
 154 sodium ion moves to cathode from the neighbor salt stream.

155 With the combination of redox couples and carbon material in Figure 1d, the release of
 156 electron and sodium ion will be greatly enhanced owing to the large active area from the
 157 carbon and more reactive sites from the redox couples on the surface of carbon material,
 158 especially with a high concentration of carbon slurry. During the charge process, the slurry in
 159 anode chamber is oxidized with the release of electron and sodium ion as shown in equation
 160 4-5.



161 At the cathode side, the mixture electrode was reduced by electrons from the outer circuit and
 162 sodium ion is accepted via CEM as shown in equation 6-7.

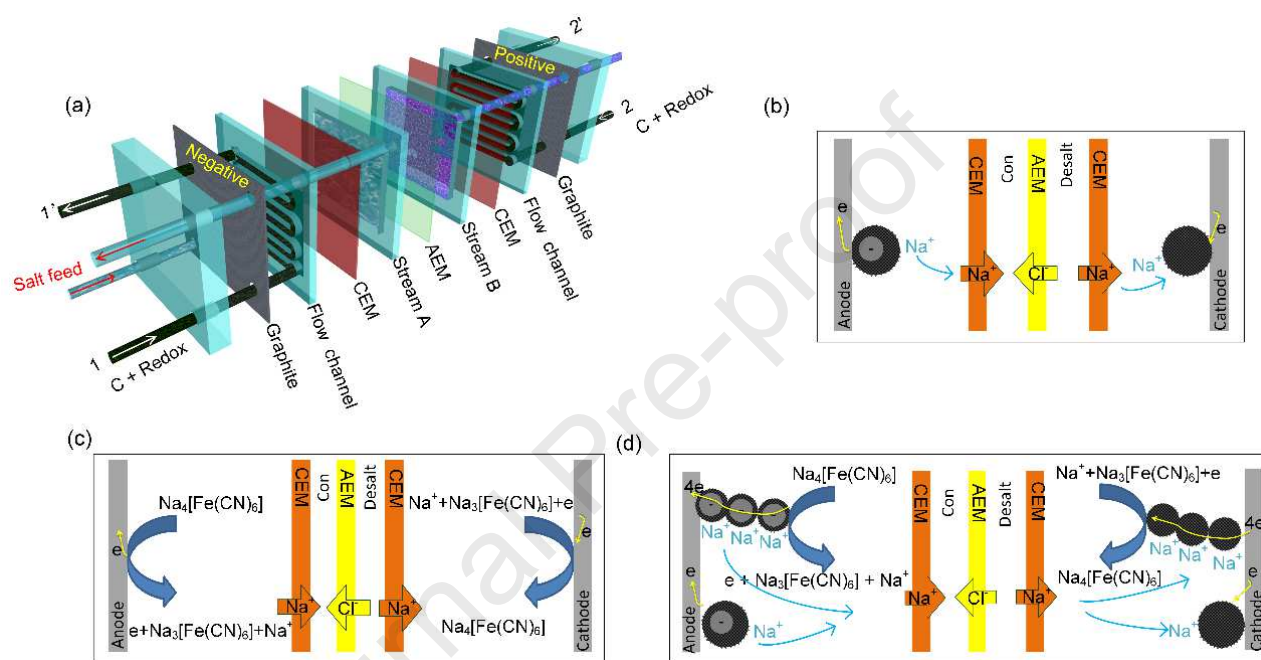


163 The ion movement in salt stream can be presented as follows:



164 The three-electrode CV of ferricyanide/ferrocyanide is displayed in Figure S2. The electrolyte
 165 was prepared with 20 mM/20 mM of ferri-/ferrocyanide with the addition of NaCl. A pair of

166 redox peaks are observed, corresponding to the electron transfer owing to the reduction and
 167 oxidation reaction. The reduction peak at 0.2 V corresponds to $[\text{Fe}(\text{CN})_6]^{3-}$ to $[\text{Fe}(\text{CN})_6]^{4-}$ and
 168 the peak at 0.26 V was assigned to oxidation reaction. The redox potential interval of 60 mV
 169 indicates the excellent redox behavior, which will be beneficial to lower down the energy
 170 consumption during electrochemical desalination[21-23].



171
 172 Figure 1. (a) Schematic representations of the FCDI cell; The proposed mechanism of FCDI
 173 with carbon material (b), the redox couple ferri-/ferrocyanide (c), and the synergetic
 174 combination of carbon and redox couples.

175

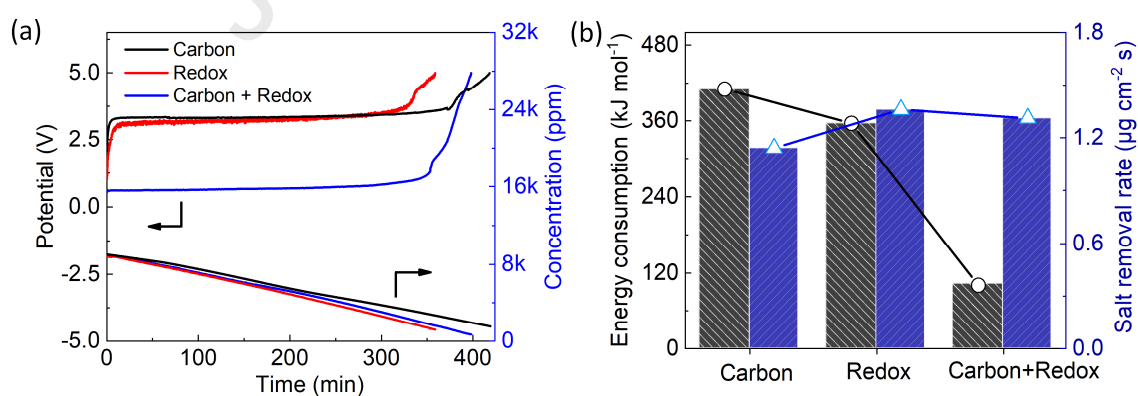
176 3.2 The enhanced desalination performance with redox couple and carbon slurry

177 To investigate the enhancement of desalination performance by combining redox couples and
 178 carbon slurry, we performed the comparison desalination tests using the redox couples or
 179 carbon slurry, separately. The results are demonstrated in Figure 2. The same current density
 180 of 2.38 mA cm^{-2} is applied. The 9 wt% AC and 1 wt% CB are dispersed in 20 mM/20 mM

181 ferri-/ferrocyanide as the flow electrode material. For AC/CB or redox couples alone, the
182 operating voltage of more than 3 V can be observed. However, the operating voltage is lower
183 down to 0.69 V with the combination of carbon slurry and redox couple, corresponding to the
184 lowest energy consumption among the tested samples. As shown in Figure 2b, the energy
185 consumption for the system with carbon slurry or redox couple is $410.26 \text{ kJ mol}^{-1}$ or 356.18 kJ
186 mol^{-1} individually. However, the energy consumption drops to $102.68 \text{ kJ mol}^{-1}$ for the system
187 with a mixture of carbon slurry and redox couple. This is attributed to the more reactive sites
188 of redox couple on the surface of carbon slurry. The released electron from ferrocyanide at the
189 anode can be easily transferred to the outer circuit, and accepted by the reduction of
190 ferricyanide at cathode chamber owing to the large active surface area of the used AC/CB. To
191 compare the electrochemical properties of carbon slurry, redox couples, or their combination,
192 we supplemented the tests of linear sweep voltammetry (LSV). As shown in Figure S3, only
193 ohmic behavior is observed in the carbon flow electrode. In the redox flow streams, the
194 limiting current can be observed from the redox reaction of ferro/ferricyanide species.
195 However, the limiting current is enhanced with the combination of carbon slurry and redox
196 flow electrode compared with bare redox couples or carbon slurry only. This may be due to
197 the more reaction sites of redox couples in the surface of carbon material. Thus, the LSV
198 electrochemical tests indicate the mixed significance of carbon slurry and redox couples in the
199 flow electrode chambers. Figure S4 shows the electrochemical impedance spectroscopy (EIS)
200 of the flow electrodes of carbon slurry, redox couples, or their combination. The surface
201 resistance (R_s) between the electrode and electrolyte in only redox couples is up to 113.7
202 ohms owing to the limited contact area on the surface of graphite paper. In the carbon slurry,
203 the R_s value drops to 57.1 ohms. However, with the combination of carbon slurry and redox
204 couples, the R_s value is down to 48.4 ohms, indicating the improved charge transfer kinetics.
205 The EIS results are consistent with the LSV data in Figure S3. In the current tests, the salt

206 removal rate in the redox couples or the mixture of redox couple and carbon slurry is slightly
 207 higher than the one in carbon even at the same current density. This may be due to the high
 208 charge efficiency in redox couples owing to the effective electron and ion transfer. In the
 209 long-term tests of the current system as shown in Figure S5, the batch cycling experiment was
 210 carried out by topping up the salt feed without the replacement of electrode materials and
 211 membranes. At the current density of 2.38 mA cm^{-2} , 9000 ppm feed salt was desalted to
 212 approximate 650 ppm level during the four cycles. The long-term tests demonstrate the
 213 excellent stability of the current desalination system, which will be applicable for multi-cycle
 214 desalination.

215 The comparison of energy consumption and salt removal rate were tabulated in Table S1,
 216 together with results obtained from the literatures. The current study displays one of the best
 217 performances with a high salt removal rate and a low energy consumption compare to other
 218 works. This high performance may be due to the improved charge transfer kinetics and the
 219 reduced interface resistance of the flow electrode to accelerate the transfer of ion and electron
 220 in FCDI.

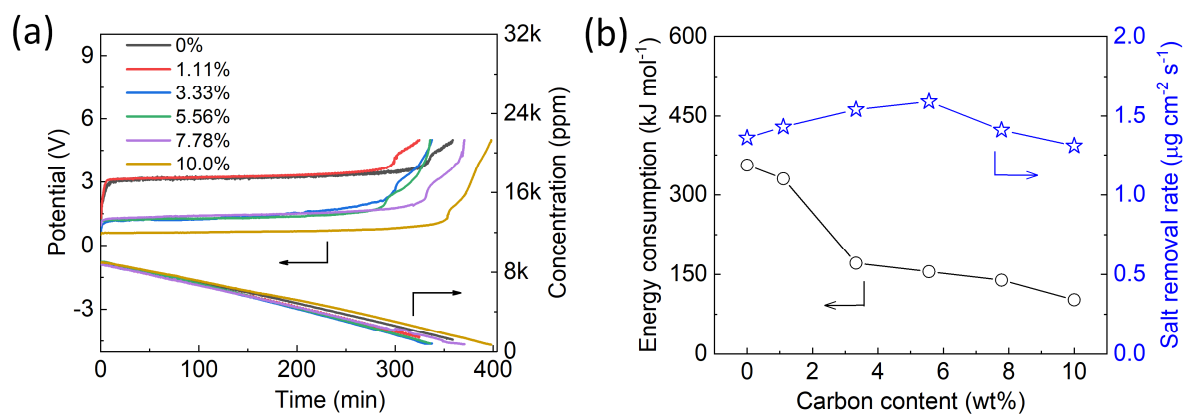


222
 223 **Figure 2.** (a) The curves of charge voltage and the corresponding variation of salt
 224 concentration in carbon slurry, redox couples, and their mixture; (b) the corresponding energy
 225 consumption and salt removal rate. The current density: 2.38 mA cm^{-2} .

226

227 **3.3 The influence of desalination performance from carbon content**

228 As discussed above, the carbon content in flow electrode can greatly affect the operating
229 voltage plateau. To investigate the influence of carbon content, the comparisons were
230 conducted with the various amount of AC/CB such as 0, 1.11, 3.33, 5.56, 7.78 and 10 wt %.
231 The ratio of AC:CB = 9:1 is kept in all the tested samples with the addition of the 20 mM/20
232 mM ferri-/ferrocyanide. The current density is 2.38 mA cm^{-2} . When the carbon mass fraction
233 is larger than 10 %, the flow ability of the electrode material is restricted, thus the maximum
234 carbon concentration is fixed at 10 % in this study. Figure 3a shows the voltage change during
235 desalination at various carbon content. The detailed voltage and concentration change in
236 diluted and concentrated streams are displayed in Figure S6. With the increase of carbon
237 content in electrode streams, the voltage declines, which further confirmed the explanation, i.e.
238 more reactive sites or contact opportunity between redox couples and carbon surface. At the
239 last stage, the voltage rises quite fast owing to the ion depletion in the diluted channel. In all
240 the experiments, the voltage was cut off at a maximum value of 5 V. The corresponding
241 energy consumption and salt removal rate are displayed in Figure 3b. When a carbon content
242 of 10 wt % is applied, the energy consumption is as low as $102.68 \text{ kJ mol}^{-1}$ and the salt
243 removal is $1.31 \text{ } \mu\text{g cm}^{-2} \text{ s}^{-1}$. With the increase of carbon content, the salt removal rate
244 increases firstly and then decreases. Among the tested samples, the best removal rate can be
245 obtained at 5.56 % carbon content as shown in Figure 3b. The key point of FCDI device is the
246 smooth flow carbon slurry between the positive and negative electrodes. When we
247 disassembled the device after desalination completion, some minor carbon slurry still
248 precipitates inside the path, which will cause the potential variation. In the future study, we
249 will further optimize the design of snake path and make the carbon slurry flow smoothly.



250

251 **Figure 3.** (a) The voltage curves with different carbon content (0, 1.11, 3.33, 5.56, 7.78 and
 252 10 wt %) and the corresponding variation of salt concentration; (b) the corresponding energy
 253 consumption and the salt removal rate. The current density: 2.38 mA cm^{-2} .

254

255 3.4 Desalination performance at various current densities

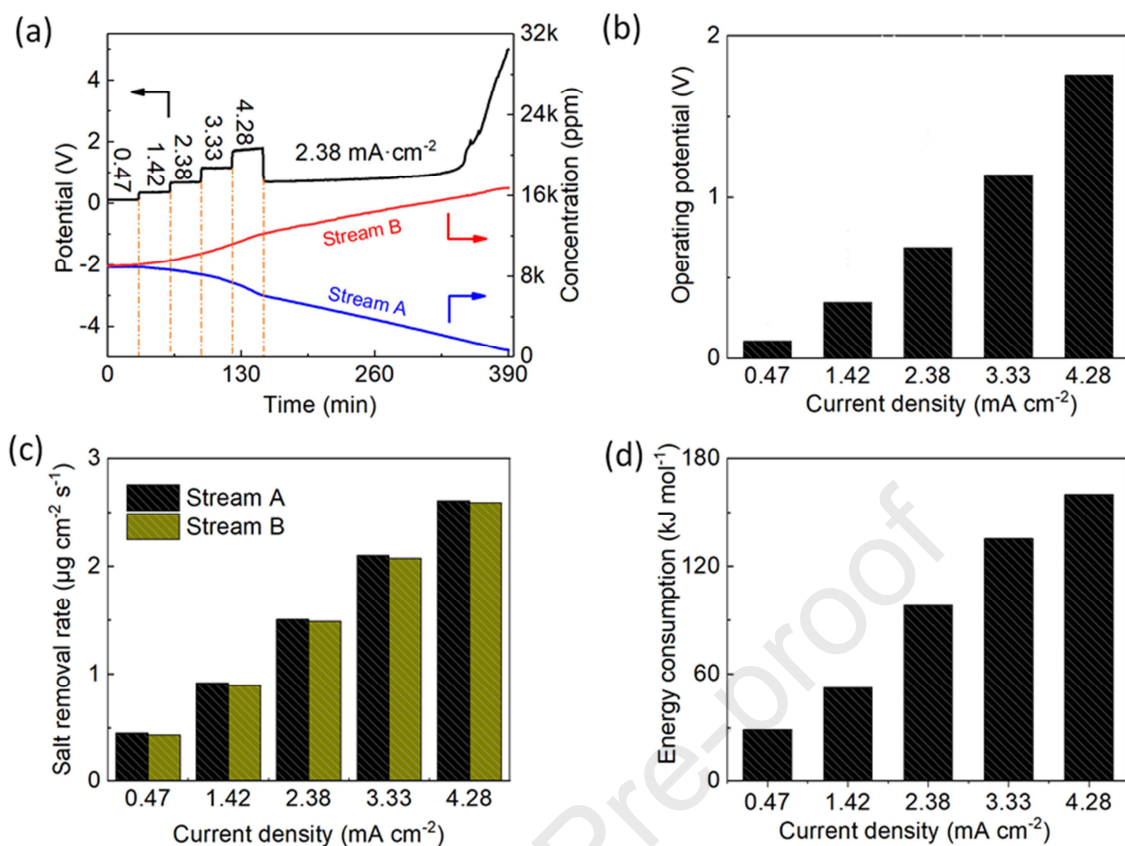
256 Further exploration was conducted on the influence of current densities on the desalination
 257 process, as shown in Figure 4. The mixture of 10 wt% AC/CB (mass ratio of 9:1) and 20
 258 mM/20 mM ferri-/ferrocyanide was used as the flow electrodes. The current densities of 0.47,
 259 1.42, 2.38, 3.33 and 4.28 mA cm^{-2} were applied. Figure 4(a) demonstrates the variations of
 260 voltage and salt content at current densities from 0.47 to 4.28 mA cm^{-2} . With the rise of
 261 current density, the voltage plateau increases as displayed in Figure 4b and Figure S7 due to
 262 the polarization. The salt removal rate depends on the applied current density in Figure 4c.
 263 The high current will drive the fast ion separation movement in both salt feeds. The removal
 264 rates in diluted channel is approximately equal to the capture rate in the concentrated reservoir.
 265 The energy consumption can be calculated from the measured the potential, current density,
 266 and removal rate. The energy consumption rises gradually with current density as shown in
 267 Figure 4d. The major reason is the increase in operating voltage with applied current. As
 268 shown in Figure 4d, in the 10 wt % carbon electrodes, the energy consumption is 52.22, 98.07,

269 135.39, 160.21 kJ mol⁻¹ at the corresponding current densities of 1.42, 2.38, 3.33 and 4.28
270 mAcm⁻² respectively.

271

272 A comparison of literature on FCDI energy consumptions and removal rates is shown in
273 Table S1 and Figure S8. For FCDI with 10 wt% DARCO and Noriactivated charcoal, the
274 energy consumption is 162.61 kJ mol⁻¹ at a current of 1.818 mA cm⁻² [20]. Reducing the
275 current to 0.909 mA cm⁻² can lower the energy consumption down to 35.79 kJ mol⁻¹. On the
276 other work, the energy consumption of 126.4 kJ mol⁻¹ can be achieved using 13 wt % YP-50F
277 activated carbon at the current of 3.0 mA cm⁻² in FCDI [24]. In the current work, the energy
278 consumption can be as low as 102.68 kJ mol⁻¹ with 20 mM/20 mM ferri-/ferrocyanide and 10
279 wt% AC/CB (mass ratio of 9:1) at a current density of 2.38 mA cm⁻² as shown in Figure 2.
280 The synergetic effect from the combination of redox couple and carbon slurry enables low
281 energy consumption and fast ion removal rate, as proved in LSV (Figure S3) and EIS (Figure
282 S4). The results in this work demonstrate a feasible method to reduce the energy consumption
283 by the introduction of redox species. Currently we are looking for other redox couples or
284 carbon material with the better desalination performance to replace the current ones.

285



286

287 **Figure 4.** (a) Desalination performance, (b) operating voltage, (c) ASRR of brine and
 288 desalinated streams and (d) energy consumption at various current densities for 10 wt%
 289 carbon content.

290

291

292 Conclusion

293 In summary, the combination of ferri-/ferrocyanide redox couple and AC/CB slurry was
 294 demonstrated as FCDI electrode to achieve a low energy consumption and high removal rate.
 295 The salt removal rate of 1.31 μg cm⁻² s⁻¹ can be obtained with 10 wt% carbon slurry and 20
 296 mM/20 mM of ferri-/ferrocyanide while the energy consumption is only 102.68 kJ mol⁻¹. The
 297 desalination performance of the electrode with combination of redox couple and carbon slurry
 298 is much better than that of the individual components alone. The excellent desalination
 299 performance is due to the synergetic effect from the combination of redox couple and carbon

300 slurry, which enables fast electron transfer and ion movement as proved by LSV and EIS. In
301 addition, the desalination performance is affected by carbon content and current densities.
302 Increasing the concentration of carbon slurry enhances salt removal. The new system with the
303 combination of redox couple and carbon slurry presented in this work will propel the
304 development of energy-saving FCDI system that can solve fresh water shortage.

305

306 **Declaration of Competing Interest**

307 The authors declare that they have no known competing financial interests or personal
308 relationships that could have appeared to influence the work reported in this paper.

309

310 **Acknowledgments**

311 This project was supported by South China Normal University, the SCNU Outstanding
312 Young Scholar Project (8S0256), the Scientific and Technological Plan of Guangdong
313 Province (2018A050506078, 2018B050502010, 2017A040405047), the Department of
314 Education of Guangdong Province (2018KTSCX047), The Scientific and Technological Plan
315 of Guangdong Province, China (2019B090905005), Natural Science Foundation of
316 Guangdong province (2019A1515011615). F. Chen acknowledges the Pearl River Talent
317 Program (2019QN01L951).

318

319

320 **References**

- 321 [1] M.A. Shannon, P.W. Bohn, M. Elimelech, J.G. Georgiadis, B.J. Mariñas, A.M. Mayes, Science and
322 technology for water purification in the coming decades, *Nature* 452(7185) (2008) 301-310.
- 323 [2] F. Duan, X. Du, Y. Li, H. Cao, Y. Zhang, Desalination stability of capacitive deionization using
324 ordered mesoporous carbon: Effect of oxygen-containing surface groups and pore properties,
325 *Desalination* 376 (2015) 17-24.
- 326 [3] M. Boota, K.B. Hatzell, M. Alhabeb, E.C. Kumbur, Y. Gogotsi, Graphene-containing flowable
327 electrodes for capacitive energy storage, *Carbon* 92 (2015) 142-149.
- 328 [4] A. Rommerskirchen, A. Kalde, C.J. Linnartz, L. Bongers, G. Linz, M. Wessling, Unraveling charge
329 transport in carbon flow-electrodes: Performance prediction for desalination applications, *Carbon*
330 145 (2019) 507-520.
- 331 [5] Y. Bouhadana, M. Ben-Tzion, A. Soffer, D. Aurbach, A control system for operating and
332 investigating reactors: The demonstration of parasitic reactions in the water desalination by
333 capacitive de-ionization, *Desalination* 268(1-3) (2011) 253-261.
- 334 [6] J. Xie, Y. Xue, M. He, W. Luo, H. Wang, R. Wang, Y.-M. Yan, Organic-inorganic hybrid binder
335 enhances capacitive deionization performance of activated-carbon electrode, *Carbon* 123 (2017)
336 574-582.
- 337 [7] S.S. Gupta, M.R. Islam, T. Pradeep, Chapter 7 - Capacitive Deionization (CDI): An Alternative Cost-
338 Efficient Desalination Technique, in: S. Ahuja (Ed.), *Advances in Water Purification Techniques*,
339 Elsevier 2019, pp. 165-202.
- 340 [8] M.E. Suss, S. Porada, X. Sun, P.M. Biesheuvel, J. Yoon, V. Presser, Water desalination via
341 capacitive deionization: what is it and what can we expect from it?, *Energy & Environmental Science*
342 8(8) (2015) 2296-2319.
- 343 [9] J. Choi, P. Dorji, H.K. Shon, S. Hong, Applications of capacitive deionization: Desalination,
344 softening, selective removal, and energy efficiency, *Desalination* 449 (2019) 118-130.
- 345 [10] Y. Cho, C.Y. Yoo, S.W. Lee, H. Yoon, K.S. Lee, S. Yang, D.K. Kim, Flow-electrode capacitive
346 deionization with highly enhanced salt removal performance utilizing high-aspect ratio
347 functionalized carbon nanotubes, *Water Res* 151 (2019) 252-259.
- 348 [11] J. Ma, J. Ma, C. Zhang, J. Song, W. Dong, T.D. Waite, Flow-electrode capacitive deionization
349 (FCDI) scale-up using a membrane stack configuration, *Water Res* 168 (2020) 115186.
- 350 [12] K. Tang, S. Yiacoumi, Y. Li, C. Tsouris, Enhanced Water Desalination by Increasing the
351 Electroconductivity of Carbon Powders for High-Performance Flow-Electrode Capacitive Deionization,
352 *ACS Sustainable Chemistry & Engineering* 7(1) (2018) 1085-1094.
- 353 [13] C. Zhang, J. Ma, T.D. Waite, The impact of absorbents on ammonia recovery in a capacitive
354 membrane stripping system, *Chemical Engineering Journal* 382 (2020) 122851.
- 355 [14] H. Yoon, J. Lee, S.-R. Kim, J. Kang, S. Kim, C. Kim, J. Yoon, Capacitive deionization with Ca-
356 alginate coated-carbon electrode for hardness control, *Desalination* 392 (2016) 46-53.
- 357 [15] P. Liang, X. Sun, Y. Bian, H. Zhang, X. Yang, Y. Jiang, P. Liu, X. Huang, Optimized desalination
358 performance of high voltage flow-electrode capacitive deionization by adding carbon black in flow-
359 electrode, *Desalination* 420 (2017) 63-69.
- 360 [16] F. Yang, J. Ma, X. Zhang, X. Huang, P. Liang, Decreased charge transport distance by titanium
361 mesh-membrane assembly for flow-electrode capacitive deionization with high desalination
362 performance, *Water Res* 164 (2019) 114904.
- 363 [17] S.-i. Jeon, H.-r. Park, J.-g. Yeo, S. Yang, C.H. Cho, M.H. Han, D.K. Kim, Desalination via a new
364 membrane capacitive deionization process utilizing flow-electrodes, *Energy & Environmental Science*
365 6(5) (2013) 1471-1475.
- 366 [18] J. Ma, D. He, W. Tang, P. Kovalsky, C. He, C. Zhang, T.D. Waite, Development of Redox-Active
367 Flow Electrodes for High-Performance Capacitive Deionization, *Environ Sci Technol* 50(24) (2016)
368 13495-13501.

- 369 [19] C. He, J. Ma, C. Zhang, J. Song, T.D. Waite, Short-Circuited Closed-Cycle Operation of Flow-
370 Electrode CDI for Brackish Water Softening, *Environ Sci Technol* 52(16) (2018) 9350-9360.
- 371 [20] J. Ma, C. He, D. He, C. Zhang, T.D. Waite, Analysis of capacitive and electrochemical contributions
372 to water desalination by flow-electrode CDI, *Water Res* 144 (2018) 296-303.
- 373 [21] F. Chen, J. Wang, C. Feng, J. Ma, T. David Waite, Low energy consumption and mechanism study
374 of redox flow desalination, *Chemical Engineering Journal* 401 (2020) 126111.
- 375 [22] E.S. Beh, M.A. Benedict, D. Desai, J.B. Rivest, A Redox-Shuttled Electrochemical Method for
376 Energy-Efficient Separation of Salt from Water, *ACS Sustainable Chemistry & Engineering* 7(15) (2019)
377 13411-13417.
- 378 [23] M.R. Gerhardt, A.A. Wong, M.J. Aziz, The Effect of Interdigitated Channel and Land Dimensions
379 on Flow Cell Performance, *Journal of The Electrochemical Society* 165(11) (2018) A2625-A2643.
- 380 [24] K.B. Hatzell, M.C. Hatzell, K.M. Cook, M. Boota, G.M. Housel, A. McBride, E.C. Kumbur, Y.
381 Gogotsi, Effect of Oxidation of Carbon Material on Suspension Electrodes for Flow Electrode
382 Capacitive Deionization, *Environmental Science & Technology* 49(5) (2015) 3040-3047.

383

Declaration of interests

The authors declare that they have no known competing financial interests or personal relationships that could have appeared to influence the work reported in this paper.

The authors declare the following financial interests/personal relationships which may be considered as potential competing interests:

Journal Pre-proof